Edward H. Herskovits, MD, PhD
Vasileios Megalooikonomou, PhD
Christos Davatzikos, PhD
Anita Chen, MS
R. Nick Bryan, MD, PhD
Joan P. Gerring, MD

Index terms:
Attention-deficit/hyperactivity disorder, 10.43
Brain, injuries, 10.43
Brain, MR, 10.121412
Children, central nervous system, 10.43
Images, analysis, 10.12149
Images, display, 10.12149

Radiology 1999; 213:389–394

Abbreviations:
ADHD = Attention-deficit/hyperactivity disorder
BRAID = brain-image database
DICA = Diagnostic Interview for Children and Adolescents
SPGR = spoiled gradient-recalled echo

[1] From the Division of Neuroradiology (E.H.H., V.M., C.D.), the Department of Biostatistics, School of Public Health (E.H.H., A.C.), and the Department of Psychiatry, Bayview Medical Center (J.P.G.), Johns Hopkins Medical Institutions, 600 N Wolfe St, Baltimore, MD 21287-7619; and the Department of Diagnostic Radiology, National Institutes of Health, Bethesda, Md (R.N.B.). From the 1998 RSNA scientific assembly. Received September 22, 1998; revision requested November 24; revision received February 24, 1999; accepted June 8. Supported in part by National Institutes of Health grant R01 AG13743-03 and by an Engines for Innovation grant from Illustra. **Address reprint requests to** E.H.H. (e-mail: *ehh@jhmi.edu*).

Author contributions:
Guarantors of integrity of entire study, E.H.H., J.P.G.; study concepts and design, R.N.B., J.P.G., E.H.H.; definition of intellectual content, E.H.H., R.N.B.; literature research, J.P.G., E.H.H.; clinical studies, J.P.G., E.H.H., R.N.B.; data acquisition, J.P.G., C.D.; data analysis, C.D., V.M.; statistical analysis, E.H.H., V.M., A.C.; manuscript preparation, E.H.H.; manuscript editing, E.H.H., J.P.G., R.N.B., C.D., V.M.; manuscript review, E.H.H., J.P.G., R.N.B.

Is the Spatial Distribution of Brain Lesions Associated with Closed-Head Injury Predictive of Subsequent Development of Attention-Deficit/Hyperactivity Disorder? Analysis with Brain-Image Database[1]

PURPOSE: To determine whether there is an association between the spatial distribution of lesions detected at magnetic resonance (MR) imaging of the brain in children after closed-head injury and the development of secondary attention-deficit/ hyperactivity disorder (ADHD).

MATERIALS AND METHODS: Data obtained from 76 children without prior history of ADHD were analyzed. MR images were obtained 3 months after closed-head injury. After manual delineation of lesions, images were registered to the Talairach coordinate system. For each subject, registered images and secondary ADHD status were integrated into a brain-image database, which contains depiction (visualization) and statistical analysis software. Using this database, we assessed visually the spatial distributions of lesions and performed statistical analysis of image and clinical variables.

RESULTS: Of the 76 children, 15 developed secondary ADHD. Depiction of the data suggested that children who developed secondary ADHD had more lesions in the right putamen than children who did not develop secondary ADHD; this impression was confirmed statistically. After Bonferroni correction, we could not demonstrate significant differences between secondary ADHD status and lesion burdens for the right caudate nucleus or the right globus pallidus.

CONCLUSION: Closed-head injury–induced lesions in the right putamen in children are associated with subsequent development of secondary ADHD. Depiction software is useful in guiding statistical analysis of image data.

Attention-deficit/hyperactivity disorder (ADHD) is a psychiatric disorder that usually manifests in early childhood and is characterized by "signs of developmentally inappropriate inattention, impulsivity, and hyperactivity" (1). ADHD frequently results in poor functioning in school and can persist into adulthood. The prevalence of ADHD is estimated at 3%–9% (2).

Research on the cause of ADHD has converged on frontostriatal dysfunction (3,4). However, there is no consensus on either the exact cause of ADHD or the mechanism by which amphetamine therapy ameliorates the symptoms and signs of ADHD (4).

Gerring et al (5) demonstrated that symptoms of ADHD develop in children after closed-head injury; these authors proposed that the diagnosis of secondary ADHD be made when a child meets psychiatric criteria for ADHD (except possibly for age of onset), with

symptoms developing after closed-head injury. It is unknown whether the same pathway that is believed to be affected in children with developmental ADHD is also affected by closed-head injury in children who develop secondary ADHD, although the distribution of lesions seen on magnetic resonance (MR) images in the setting of closed-head injury does overlap with the neuronal pathways implicated in developmental ADHD.

The widespread availability of MR examination of the brain has led to detailed description of the imaging findings associated with closed-head injury, such as shear injury and contusion (6). Neuroimaging studies have demonstrated differences in total cerebral volume and basal ganglia volume in children with developmental ADHD (4). The primary purpose of this study was to determine whether the spatial distributions of closed-head injury–induced brain lesions detected at MR examination of the brain differ in children who do or do not subsequently develop secondary ADHD. In particular, we formulated three null hypotheses regarding differences between the group of children who develop secondary ADHD and the group of children who do not develop secondary ADHD:

1. The two groups do not differ with respect to degree of involvement of the right caudate nucleus.
2. The two groups do not differ with respect to degree of involvement of the right globus pallidus.
3. The two groups do not differ with respect to degree of involvement of the right putamen.

MATERIALS AND METHODS

Determination of ADHD Status: Post–Closed-Head Injury Behavioral Study

We obtained the data for this work from an ongoing study by Gerring et al (5) of post–closed-head injury personality changes in which the researchers prospectively examine children referred from tertiary trauma centers to a university-affiliated center (Kennedy Krieger Institute, Baltimore, Md, affiliated with Johns Hopkins Medical Institutions, Baltimore, Md) for treatment of children with neurologic disorders. All subjects were approved by the Joint Committee on Clinical Investigation, Johns Hopkins Medical Institutions. At least one parent or legal guardian for each subject provided written informed consent before inclusion in the study. One child's family declined participation in the study. Exclusion criteria for study entry included previous hospitalization or emergency room visits for closed-head injury; premorbid mental retardation; documented child abuse; and premorbid neurologic conditions, such as seizure disorder. The study cohort consisted of 99 children aged 4–19 years. Eighty-nine children had had severe closed-head injury (Glasgow coma scale [7,8] score of 3–8), and the remaining 10 children had had moderate closed-head injury (Glasgow coma scale score of 9–12).

The study protocol included assessment of premorbid (ie, pre–closed-head injury) ADHD status by administering the Diagnostic Interview for Children and Adolescents (DICA)(5) to parents on the day of enrollment into the study (mean of 20 days after closed-head injury). Similarly, ADHD status 1 year after injury was determined by readministering the DICA to the parent. This process and its validity in this setting are described in greater detail in the article by Gerring et al (5).

Of the children who did not have ADHD at baseline as determined by administering the DICA to their parents, two clinical subgroups were identified for the purposes of this study: children who did not develop secondary ADHD, and those who subsequently did develop secondary ADHD when the DICA was administered to their parents 1 year after injury. For the purposes of this study, we excluded the 19 children who had ADHD at baseline and the child whose family would not provide informed consent for MR examination, for a total of 79 remaining subjects.

Delineation of Brain Lesions: MR Image Acquisition and Processing

Because of research findings that indicate that MR examination immediately after closed-head injury may not be as useful prognostically as examination 3 months after injury (9), Gerring et al (5) chose 3 months as the target interval between closed-head injury and MR examination. Subjects underwent MR examination a mean of 104 days after injury. At the time of MR examination, all children's conditions were clinically stable; approximately half of the children were outpatients, and the remainder were receiving neurorehabilitation therapy at the Kennedy Krieger Institute. Fifty-five (70%) of the 79 subjects were trained to inhibit motion through an operant conditioning procedure (10); the remaining 24 subjects (30%) were sedated with intravenous administration of 4 mg of pentobarbital sodium (Nembutal Sodium; Wyeth Pharmaceuticals, Philadelphia, Pa) per kilogram of body weight. All studies were monitored by one of the investigators, and sequences were repeated as necessary for motion degradation.

MR examination of the brain included a T1-weighted (500/20 [repetition time msec/echo time msec], one signal acquired) sagittal localizing sequence with 5-mm section thickness, 1.5-mm section gap, 24-cm field of view, and 192 × 256 matrix. Midsagittal images were used to identify the anterior commissure–posterior commissure line, along which all oblique transverse images were oriented. Spin-echo spin-density-weighted (3,000/30, one-half signal acquired) and T2-weighted (3,000/100, one-half signal acquired) oblique transverse images with 5-mm section thickness, no section gap, 20-cm field of view, and 192 × 256 matrix were acquired from the vertex to the foramen magnum. T1-weighted spoiled gradient-recalled-echo (SPGR; 35/7, 45° flip angle, one signal acquired) oblique transverse images with 1.5-mm section thickness, no section gap, 24-cm field of view, and 128 × 256 matrix were acquired from the vertex to the foramen magnum on 1.5-T (GE Medical Systems, Milwaukee Wis) instruments at one site.

To our knowledge, prior literature does not definitively document which MR pulse sequence is the most sensitive to the chronic lesions seen in children after closed-head injury; in contrast to the acute setting, in which T2-weighted images demonstrate associated edema, most authors agree that high-spatial-resolution images with T2* sensitivity are recommended in the chronic setting, particularly for small lesions, such as those seen after axonal-shear injury (11). With respect to lesion characterization, the goal of this study was the delineation of chronic lesions rather than the specification of the type of injury for each lesion. Given that the most common lesions in this study are axonal-shear injuries and contusions and that the T1-weighted SPGR sequence has high spatial resolution and T1- and T2*-contrast sensitivity, we chose images from this sequence for manual delineation of the closed-head injury lesions. We confirmed this choice by performing a preliminary comparison of the T2-weighted images with the T1-weighted SPGR images in two subjects, for which we found more lesions on the SPGR images.

The volumetric T1-weighted images were displayed on a 1,024 × 1,024-pixel workstation and were evaluated by two

independent, trained readers (one experienced neuroradiologic technologist and one physician [J.P.G.]) who were blinded to information about the subjects. Rather than specify the location of each lesion, each reader manually delineated as a region of interest each intraaxial region of signal intensity abnormality, either hypo- or hyperintensity, for each volumetric T1-weighted image. These abnormalities included hematoma, contusion, infarct, and axonal-shear injury and were generically designated as ''lesions.''

A senior board-certified radiologist with subspecialty neuroradiologic training (R.N.B.) adjudicated each of these readings. Iatrogenic lesions, such as ventriculostomy-catheter tracks, were specifically excluded from the analysis by the readers and the adjudicator. Regions of interest were reconstructed into three-dimensional structures. Lesion volumes were computed by using proprietary software (ALLEGRO; ISG, Toronto, Canada).

Image data were registered to the Talairach stereotaxic reference frame (12) by using nonlinear elastic-deformation software (13). Because the accuracy of registration of subjects' images to a common standard directly affects the quality of subsequent statistical analysis, we had previously evaluated this algorithm for registration error by using images acquired with MR parameters identical to those used to acquire images for this study. This analysis yielded an estimate of 3.4-mm mean registration error (2.1-mm SD) for cortical structures and 2.5-mm mean registration error (1.6-mm SD) for subcortical structures (13).

Data Analysis: Brain-Image Database

Each subject's image and clinical data were integrated into our brain-image database (BRAID), which is an object-relational database that has been designed and implemented by using Illustra (Illustra, Oakland, Calif), a commercial object-relational database management system; the database was run on an Impact workstation (Silicon Graphics, Mountain View, Calif). The primary goal of the BRAID project was to facilitate image-based clinical trials by seamlessly integrating image-processing and statistical operators into a database management system. BRAID has a structured query language interface (14), which allows users to select arbitrary subgroups of subjects for further analysis or for display.

Standard database management systems cannot recognize, much less analyze or display, image data. Using the object-relational model, we extended the Illustra database management system by incorporating image-processing and display operators into BRAID. For example, we implemented a summation operator for images, which allowed us to view images of lesions summed over an arbitrary subgroup of subjects; each voxel in a summary image is a histogram bin, which contains the number of subjects for whom this voxel was abnormal. We also incorporated several digital brain atlases into BRAID; examples include the stereotaxic atlas of Talairach and Tournoux (12), the Brodmann atlas (15,16), and a synthetic atlas that contains regions of interest that we delineated. BRAID's image-processing routines are invoked via its structured query language interface; similarly, these atlases can be displayed by using structured query language statements.

Just as standard database management systems lack image-processing operators, they provide only simple tabulation and arithmetic functions for analyzing or summarizing data. We extended these arithmetic facilities by incorporating statistical operators into BRAID so that we could analyze image data and clinical variables for associations. For example, we implemented modules that compute the χ^2 and Fisher exact test statistics, invoked by means of BRAID's structured query language interface.

BRAID's operations can be divided into three functional modes: visualization, in which summary images for subgroups of subjects are presented on the basis of structured query language queries; analysis, in which statistics are computed to compare images and clinical variables for subgroups of subjects, again on the basis of structured query language queries; and exploration, in which BRAID computes statistics that compare all pairwise combinations of atlas structures and clinical variables and returns a list of associations among clinical and image variables sorted by *P* value.

After images were registered to a common coordinate system, they and the corresponding clinical data were integrated into BRAID for further analysis. Summation images of all lesions over all subjects in each subgroup were obtained and examined visually. On the basis of these images and previous research findings that implicate a frontostriatal pathway in the cause of ADHD, we chose for further analysis three atlas structures that corresponded to the three hypotheses listed in the first section. For each atlas structure analyzed, two statistical approaches were applied; the first was based on discrete image variables, and the second was based on continuous image variables.

We began with a three-dimensional atlas structure (eg, right globus pallidus) for each subject. If the structure intersected any of that subject's lesions, we labeled the structure as abnormal; otherwise, we labeled the structure as normal. For each atlas structure, we used BRAID to construct a 2×2 contingency table to determine whether the status of that atlas structure (ie, normal vs abnormal) was associated with secondary ADHD status (ie, present vs absent) 1 year after injury. Due to low expected frequencies for several cells in these contingency tables, we used BRAID to compute two-tailed Fisher exact test statistics (17) and applied the Bonferroni correction (for three hypotheses) to these results.

In labeling a structure as abnormal if there were any overlap with lesions, we effectively used a threshold of 0 voxels for labeling a structure as normal or abnormal. In fact, there is no widely accepted rule for setting this threshold, and it is almost certainly the case that some structures function normally even with relatively large lesions, while others do not function normally even with small lesions.

To remove the effects of thresholding, we also analyzed atlas structures as continuous variables. For this analysis, we again started with an image for each atlas structure that intersected with a particular subject's image data. For each structure, we computed the fraction of its volume that overlapped with the subject's lesions; we will refer to this quantity as the ''lesion fraction.'' Thus, if the structure did not intersect with the subject's lesions, the lesion fraction was 0 (equivalent to labeling it ''normal'' for contingency-table analysis); if half of the atlas structure intersected that subject's lesions, the lesion fraction was 0.5; and so on. Because the distributions of these fractions are not Gaussian, we computed the independent-sample two-tailed Mann-Whitney statistic to detect associations among the lesion fraction and the secondary ADHD status, and we applied the Bonferroni correction for the number of hypotheses. In addition to visualization and directed statistical analysis, we used BRAID to perform an exploratory analysis of these data, with examination of all noncortical Talairach atlas structures to determine the association of lesion fraction with secondary ADHD status. We excluded all atlas structures from this analysis that were represented as surfaces, such as gyri and claustrum, since

a registration error of even 1 mm could dramatically affect results for these structures.

RESULTS

Of the 80 subjects without ADHD at baseline, one subject's family declined to provide informed consent for MR examination, and three subjects had incomplete MR data sets due to transmission or storage errors; clinical data (ie, DICA results) were available for all subjects. Of the 76 subjects included in this analysis, 15 (20%) developed secondary ADHD and 61 (80%) did not. As reported by Gerring et al (5), significant differences between these groups could not be demonstrated with respect to the Glasgow Coma Scale, total numbers of lesions, and total lesion volumes. In addition, significant differences between these groups could not be demonstrated with respect to age, sex, neurosurgical intervention, or treatment with behavior-altering medications. Only four children were left-handed, none of whom developed secondary ADHD. After adjudication, the readers identified 1,173 lesions; interreader agreement was 72% (846 of 1,173 lesions). After constructing the database of lesions and clinical data, we examined axially reformatted summary images of the subjects, which is similar to the procedure we had previously employed in visualizing a subset of the Cardiovascular Health Study data (18).

Figure 1 shows two representative transverse images with lesions summed over all 76 subjects. By submitting more complex structured query language statements to BRAID, we can obtain equivalent images for subsets of interest. For example, Figures 2 and 3 show the same transverse levels with summed lesions for subjects who did not and for subjects who did develop secondary ADHD, respectively. Note that the right putamen appears to be more extensively involved in subjects who developed secondary ADHD, whereas the frontal lobes and left putamen appear to be more commonly involved in subjects who did not develop secondary ADHD.

We confirmed the results of visualization statistically, as shown in Tables 1 and 2. Although none of the Fisher exact test statistics corresponding to the three hypotheses reach significance after Bonferroni correction, the Bonferroni-corrected Mann-Whitney statistics indicate an association between lesion fraction in the right putamen at 3 months and secondary ADHD status at 1 year. The Mann-Whitney statistic for the right caudate nucleus approaches, but does not reach, significance after Bonferroni correction. In contrast, we could not demonstrate an association between lesion fraction in the right globus pallidus and development of secondary ADHD.

Finally, we performed an exploratory (post hoc) analysis of all remaining Talairach atlas structures; however, only the left thalamic hemisphere (uncorrected Fisher exact test, $P = .035$; Mann-Whitney test, $P = .022$) yielded a P value less than or equal to .05 when analyzed for association with development of secondary ADHD.

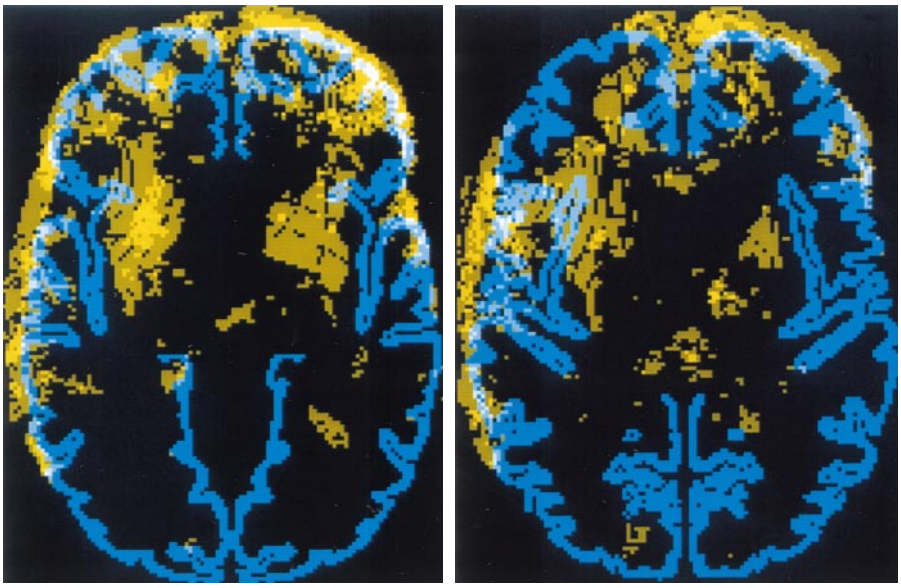

a. **b.**

Figure 1. Transverse summary images at the level of the **(a)** basal ganglia and **(b)** thalamus for all lesions in all 76 subjects with MR data sets. The lesions are yellow, and the Talairach cortex is blue.

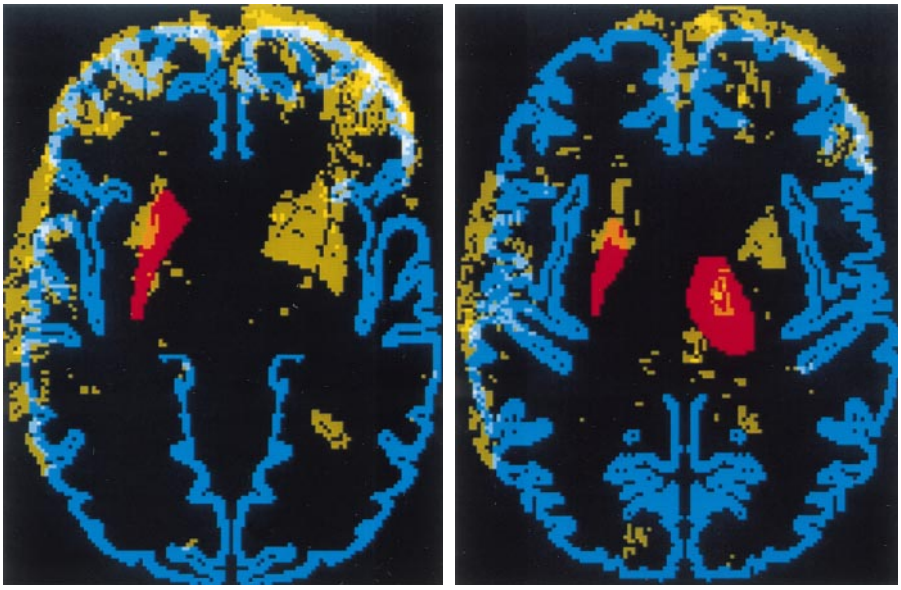

a. **b.**

Figure 2. Transverse summary images at the level of the **(a)** basal ganglia and **(b)** thalamus for all lesions in the 61 subjects with MR data sets who did not develop secondary ADHD. The lesions are yellow, the Talairach cortex is blue, and the right putamen and left thalamic hemisphere are red.

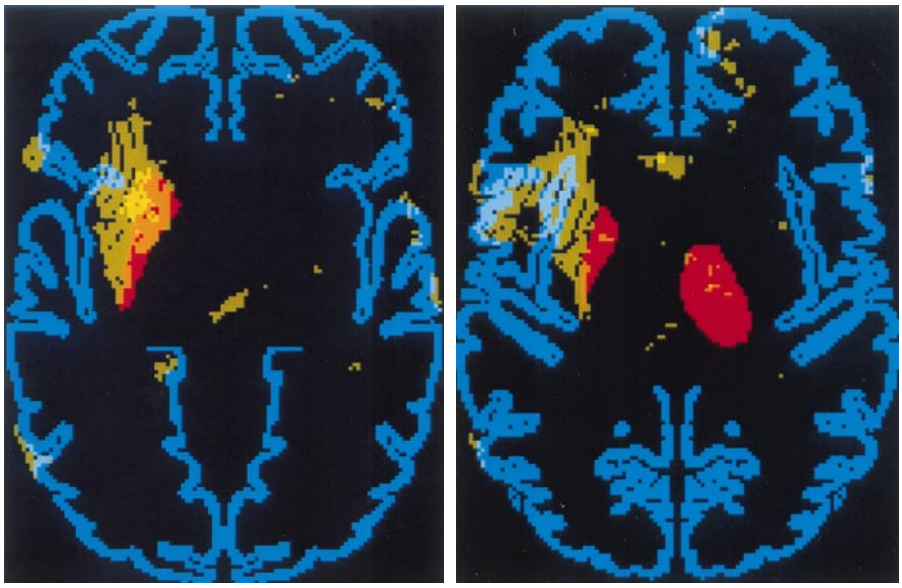

a. b.

Figure 3. Transverse summary images at the level of the **(a)** basal ganglia and **(b)** thalamus for all lesions in the 15 subjects who developed secondary ADHD. The lesions are yellow, the Talairach cortex is blue, and the right putamen and left thalamic hemisphere are red.

TABLE 1
Association of Atlas Structure Status with Secondary ADHD Status

Structural Variable*	Fisher Exact Test *P* Value†
Right caudate nucleus	.049
Right putamen	.022
Right globus pallidus	.337

* An atlas structure is labeled "normal" if it does not intersect with any of a subject's lesions; otherwise, the structure is labeled "abnormal" (see Materials and Methods for details).

† A *P* value less than the Bonferroni-corrected significance value of (0.05/3) = .017 is considered to indicate a significant difference.

TABLE 2
Association of Atlas Structure Lesion Fraction with Secondary ADHD Status

Structural Variable*	Mann-Whitney Test *P* Value†
Right caudate nucleus	.018
Right putamen	.008
Right globus pallidus	.603

* A lesion fraction of an atlas structure is the fraction of that structure's volume that intersects a subject's lesions (range, 0–1; as described in Materials and Methods).

† A *P* value less than the Bonferroni-corrected significance value of (0.05/3) = .017 is considered to indicate a significant difference.

DISCUSSION

In comparing children who develop secondary ADHD 1 year after closed-head injury with those who do not, we have shown that the spatial distributions of closed-head injury–induced lesions seen on MR images differ in these two groups. In particular, children who develop secondary ADHD tend to have higher lesion fractions in the right putamen than children who do not develop secondary ADHD. Results for the right caudate nucleus are suggestive of an association with secondary ADHD but do not reach significance after Bonferroni correction. Exploratory data analysis yielded only the left thalamic hemisphere as an additional potentially important structure in the cause of secondary ADHD. In contrast to the literature on developmental ADHD, we could find no evidence of an association between lesions in the right globus pallidus and development of secondary ADHD. This difference may reflect underlying differences in the causes of developmental ADHD and secondary ADHD and may provide a starting point for investigation into the differences between these entities. Of interest, anatomic studies of children with developmental ADHD demonstrate loss of volume of frontal and striatal structures but no lesions; thus, ADHD may be a manifestation of any injury to the striatum, as opposed to a (solely) developmental disorder.

Although cortical structures, particularly those in the frontal lobes, are prominent components of hypothesized pathways involved in developmental ADHD, our atlas structures and registration methods are not currently adequate for analyses of cortical structures, because these structures are surfaces (ie, cortex) rather than volumes and are thus strongly affected by minimal registration error. The relative lack of frontal lesions in the group that developed secondary ADHD indicates a potentially important difference between this group and children with developmental ADHD. Much more is known about cortical function than about the functional anatomy of white matter tracts, which biases atlases in favor of the former; however, we are in the process of constructing an atlas that contains structures consisting of cortex and adjacent subcortical white matter. It remains to be seen whether these new atlas structures will enable us to detect associations among gyral lesions and clinical variables. Clearly, visualization (Figs 2, 3) demonstrates prominent frontal-lobe differences between the two groups; it is curious that frontal lesions seem to predict nondevelopment of secondary ADHD, which again contradicts findings in children with developmental ADHD.

An important confounding factor in this analysis is the distribution of lesions in closed-head injury; even if a structure were a critical component of the hypothesized ADHD pathway, we would not be able to evaluate it if closed-head injury only rarely caused lesions in that structure. For example, one possible reason for our having detected an association of right putamen lesions but not right caudate nucleus lesions in cases of secondary ADHD is the relatively small number of lesions intersecting the right caudate nucleus (five lesions vs 10 lesions for the right putamen). Similarly, to the extent that closed-head injury produces bilaterally symmetric frontal-lobe injury (and concomitant temporal lobe injury), several structures may be spuriously associated with secondary ADHD, if, in fact, the right frontal lobe plays a prominent role in the development of ADHD. It is important to note that none of the iatrogenic lesions (ie, ventriculostomy catheter tracks) traversed the basal ganglia; thus, we did not affect the analyses of these structures by excluding iatrogenic lesions from this study.

An important limiting factor of atlas-based analysis of brain images is the

quality of registration, particularly for small or thin atlas structures, such as cortex. We discussed this problem in greater detail in a previous article (18) and have since improved our registration methods from piecewise-linear registration to nonlinear, elastic deformation based on surfaces of ventricles and gyri (13). Even so, we have previously shown that registration errors of only a few millimeters can lead to loss of sensitivity and specificity, particularly for surfaces, such as cortex (18). Clearly, Figures 1 and 2 demonstrate that some cortical contusions appear to lie outside of the brain after registration, which impedes analysis of frontal-lobe structures. Also, even the 2.5-mm mean registration error that we reported for subcortical structures (13) would affect the registration of small structures, such as the caudate nucleus, that are central to ADHD research. Since we expect to continue to improve our registration algorithm, the statistical power of our methods should only increase in the future.

Although sample size in this study is comparable to or greater than that in other ADHD studies, this lesion-deficit analysis is somewhat limited by the relatively small number of subjects and by the relatively high prevalence of ADHD at baseline (19% [19 of 99 subjects]). Although we cannot compute the exact sample size required for the Mann-Whitney test, we can approximate these power calculations by using sample-size estimates for 2×2 contingency tables. For example, for subjects who did not develop secondary ADHD, the probability of having left thalamic lesions is approximately 0.10 (six of 61 patients), and for subjects who developed secondary ADHD, the probability of having left thalamic lesions is approximately 0.33 (five of 15 patients). If we want to be able to detect this difference in lesion burden with an α of 0.05 and a β of 0.2 (19), we would require approximately 30 subjects for each group, which is twice the number of subjects currently enrolled in the group that developed secondary ADHD.

It is encouraging that, despite these limitations, we have found preliminary evidence that the frontostriatal pathway that is implicated in the cause of developmental ADHD is also involved in secondary ADHD. Our demonstration of an association between lesions in the right striatum and development of secondary ADHD confirms similar findings described for developmental ADHD (4). It is also noteworthy that the left thalamic hemisphere, which is also implicated in the cause of developmental ADHD, shows evidence of association with secondary ADHD in this study, which provides a promising area of focus for future studies.

We have also shown that BRAID, our software workbench for supporting the analysis of image-based clinical trials, can produce clinically meaningful results from data sets that were gathered completely independently of the design and implementation of BRAID. As more subjects are examined as part of the secondary ADHD study, it will be relatively simple for us to reanalyze the data, either statistically or for visual presentation. Similarly, if we come across a new anatomic hypothesis regarding the cause of ADHD in the literature, we can easily analyze the corresponding atlas structure or construct and analyze a new structure if necessary. In addition, BRAID's generalized architecture will allow us to analyze data from other image-based clinical trials, regardless of imaging modality.

Acknowledgment: We thank Cynthia B. Wursta, RT, for assistance with reading MR images.

References

1. American Psychiatric Association. Diagnostic and statistical manual of mental disorders. 3rd ed. Washington, DC: American Psychiatric Association, 1987.
2. Richters JE, Arnold LE, Jensen PS, et al. NIMH collaborative multisite multimodal treatment study of children with ADHD. I. Background and rationale. J Am Acad Child Adolesc Psychiatry 1995; 34:987–1000.
3. Cummings JL. Frontal-subcortical circuits and human behavior. Arch Neurol 1993; 50:873–880.
4. Castellanos FX. Neuroimaging of attention-deficit hyperactivity disorder. Child Adolesc Psychiatr Clin North Am 1997; 6:383–411.
5. Gerring JP, Brady KD, Chen A, et al. Premorbid prevalence of attention-deficit hyperactivity disorder and development of secondary attention-deficit hyperactivity disorder after closed-head injury. J Am Acad Child Adolesc Psychiatry 1998; 37: 647–654.
6. Gentry LR, Godersky JC, Thompson B. MR imaging of head trauma: review of the distribution and radiopathologic features of traumatic lesions. AJR 1988; 150:663–672.
7. Teasdale G, Jennett B. Assessment of coma and impaired consciousness: practical scale. Lancet 1974; 2:81–84.
8. Teasdale GM, Pettigrew LE, Wilson JT, Murray G, Jennett B. Analyzing outcome of treatment of severe head injury: a review and update on advancing the use of the Glasgow Outcome Scale. J Neurotrauma 1998; 15:587–597.
9. Wilson JT. The relationship between neuropsychological function and brain damage detected by neuroimaging after closed head injury. Brain Inj 1990; 4:349–363.
10. Slifer KJ, Cataldo MF, Cataldo MD, Llorente AM, Gerson AC. Behavior analysis of motion control for pediatric neuroimaging. J Appl Behav Anal 1993; 26:469–470.
11. Gentry LR. Imaging of closed head injury. Radiology 1994; 191:1–17.
12. Talairach J, Tournoux P. Co-planar stereotaxic atlas of the human brain. Stuttgart, Germany: Thieme, 1988.
13. Davatzikos C. Spatial transformation and registration of brain images using elastically deformable models. Comput Vision Image Understanding 1997; 66:207–222.
14. Chamberlain DD, Astrahan MM, Eswaran KP, et al. Sequel 2: a unified approach to data definition, manipulation, and control. IBM J Res Dev 1976; 20:560–575.
15. Brodmann K. Vergleichende lokalisationslehre der grosshirnrinde. Leipzig, Germany: Barth, 1909.
16. Nowinski WL, Bryan RN, Raghavan RE, eds. The electronic clinical brain atlas on CD-ROM. Stuttgart, Germany: Thieme, 1997.
17. Andres AM, Tejedor IH. On conditions for validity of the approximations to Fisher's exact test. Biometrical J 1997; 39:935–954.
18. Letovsky SI, Whitehead SHJ, Paik CH, et al. A brain image database for structure/function analysis. AJNR 1998; 19:1869–1877.
19. Fisher LD, van Belle G. Biostatistics: a methodology for the health sciences. New York, NY: Wiley, 1993.